actuators

MDPI

Article

Core–Shell Droplet Generation Device Using a Flexural Bolt-Clamped Langevin-Type Ultrasonic Transducer †

Kentaro Omori, Nozomu Fujimoto, Takefumi Kanda *, Shuichi Wakimoto and Norihisa Seno

Graduate School of Natural Science and Technology, Okayama University, 3-1-1 Tsushima-Naka, Kita-ku, Okayama 700-8530, Japan; oomori18@s.okayama-u.ac.jp (K.O.); fujimoto15@s.okayama-u.ac.jp (N.F.); wakimoto@okayama-u.ac.jp (S.W.); senoh-n@cc.okayama-u.ac.jp (N.S.)

* Correspondence: kanda-t@okayama-u.ac.jp

† This paper is based on conference presentation, K. Omori, N. Fujimoto, T. Kanda, S. Wakimoto, N. Seno: "Core-shell droplet generation device using a flexural vibration by a bolt-clamped Langevin type ultrasonic transducer". ACTUATOR 2021, International Conference and Exhibition on New Actuators and Drive Systems, Online, 17–19 February 2021.

Abstract: Droplets with a core–shell structure formed from two immiscible liquids are used in various industrial field owing to their useful physical and chemical characteristics. Efficient generation of uniform core–shell droplets plays an important role in terms of productivity. In this study, monodisperse core-shell droplets were efficiently generated using a flexural bolt-clamped Langevin-type transducer and two micropore plates. Water and silicone oil were used as core and shell phases, respectively, to form core–shell droplets in air. When the applied pressure of the core phase, the applied pressure of the shell phase, and the vibration velocity in the micropore were 200 kPa, 150 kPa, and 8.2 mm/s, respectively, the average diameter and coefficient of variation of the droplets were 207.7 μm and 1.6%, respectively. A production rate of 29,000 core–shell droplets per second was achieved. This result shows that the developed device is effective for generating monodisperse core–shell droplets.

Keywords: core-shell droplet; microfluidic device; ultrasonic transducer

Citation: Omori, K.; Fujimoto, N.; Kanda, T.; Wakimoto, S.; Seno, N. Core–Shell Droplet Generation Device Using a Flexural Bolt-Clamped Langevin-Type Ultrasonic Transducer. *Actuators* **2021**, *10*, 55. https://doi.org/10.3390/act10030055

Received: 18 February 2021
Accepted: 7 March 2021
Published: 9 March 2021

1. Introduction

Droplets with core–shell structures formed from two immiscible liquids have useful physical and chemical characteristics, such as protection of the core phase by the shell phase, simultaneous use of two substances, and improved shell phase reactivity using the core phase as a catalyst. Therefore, core–shell droplets are commonly used in industrial fields such as medicine, cosmetics, and food. Many studies using core–shell droplets have been reported [1–5], wherein it is necessary to manage each droplet that is generated. Thus, the efficient generation of uniform core–shell droplets has an important role in terms of productivity, and is a topic of considerable research interest [6–17].

A large number of core–shell droplets can be simultaneously generated by membrane emulsification [6]. This method is categorized bulk method. However, this method cannot control the generation of each droplet, and two-step emulsification is required.

A microfluidic device composed of glass capillaries is a typical device used for generating core–shell drop-lets [7–11]. The droplets are generated individually in the microchannel, achieving a production rate of thousands of droplets per second.

Core–shell droplets have a complex structure and are more difficult to generate than single droplets. Thus, an efficient core–shell droplet generation method is required. Monodisperse single droplets have been efficiently generated using vibration-based methods [18–22]. It is possible to generate tens of thousands of droplets per second, which is the production rate of droplets required for core-shell droplet generation with high

efficiency. Among the flow methods that generate droplets one by one, the vibration-based method has high generation efficiency.

In the present study, monodisperse core–shell droplets were generated by a vibration method. A core–shell droplet generation device using a bolt-clamped Langevin-type flexural transducer and two micropore plates was designed.

2. Design and Fabrication

2.1. Droplets Generation Principle

The principle behind the droplet generation in this research is surface tension. Fluid is converted into droplets by surface tension. This method used relies on electric power to turn fluid into droplets with controlled size. In addition, production rate of droplets is controlled using vibration [18–22].

First, the supplied fluid is ejected from the micropore to air. The ejected jet flow breaks under the effect of surface tension and turns into droplets. When vibration is not applied, uniform droplets are not generated. Conversely, when vibration is applied, uniform droplets are generated. Vibration is applied vertically to the flow direction of the jet flow. Uniform waves with the same period as the vibration are generated on the surface of the jet flow. The driven frequency is equal to the number of droplets.

A double-structure jet flow is necessary for core–shell droplet generation. This double-structure jet is a coaxial flow in which the core phase is covered by a shell phase, thereby generating core–shell droplets as they exit the device.

2.2. Structure

Figures 1 and 2 show the schematic and photograph of the core–shell droplet generation device, respectively. The length of the device is 42.7 mm and the diameter is 18 mm. A bolt-clamped Langevin-type ultrasonic transducer was used to obtain flexural vibration. Piezoelectric elements (PZT) polarized in the thickness direction are sandwiched between metal blocks.

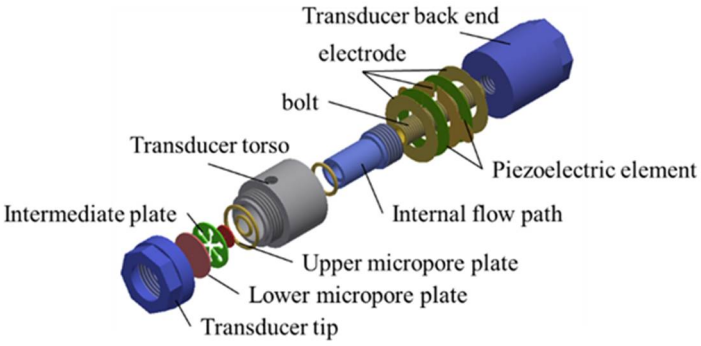

Figure 1. Schematic of the core–shell droplet generation device.

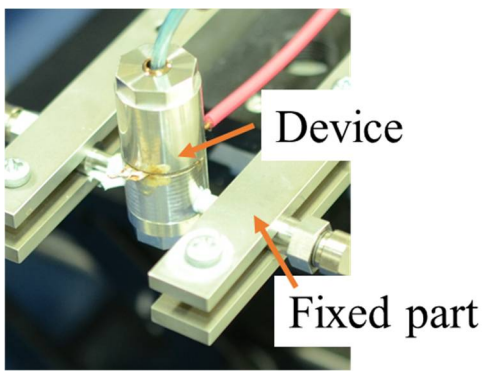

Figure 2. Photograph of the core–shell droplet generation device.

To discharge a double-structure jet flow, the device has a channel part at the tip of the device.

As shown in Figure 3, the channel part is assembled to three plates: an upper plate, an intermediate plate, and a lower plate. The intermediate plate is sandwiched between the upper and lower plates to provide a shell phase flow path. The upper and lower micropore diameters are 50 μm and 100 μm, respectively. The schematic of the upper micropore plate for the core–shell droplet generation device is shown in Figure 4. The micropore plate is 6 mm in diameter and 0.5 mm thick. A schematic for the lower micropore plate for the core–shell droplet generation device is shown in Figure 5. The micropore plate is 12 mm in diameter and 0.5 mm thick. Figure 6 shows the cross section of the device. The core phase supplied from the top of the device is injected into the shell phase supplied from the side to generate the core–shell two phase flow.

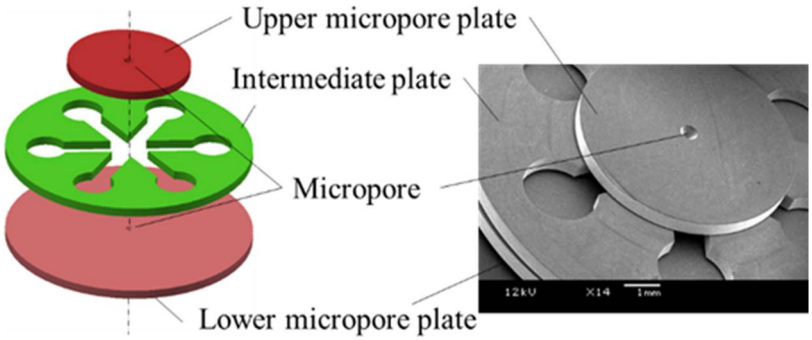

Figure 3. Channel part with stacked micropore plates: (**a**) schematic of channel part; (**b**) channel part SEM image.

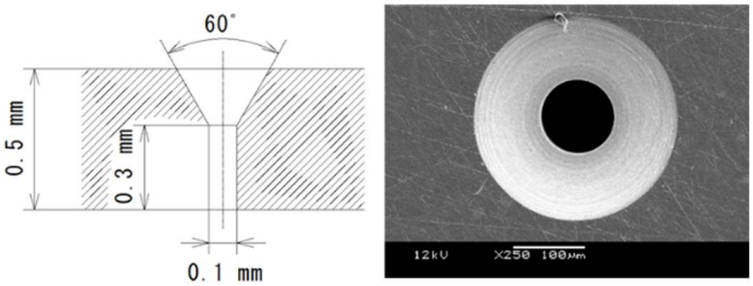

Figure 4. Schematic of upper micropore plate for core–shell droplet generation device: cross-sectional view of micropore (**left**) and SEM photograph of micropore (**right**).

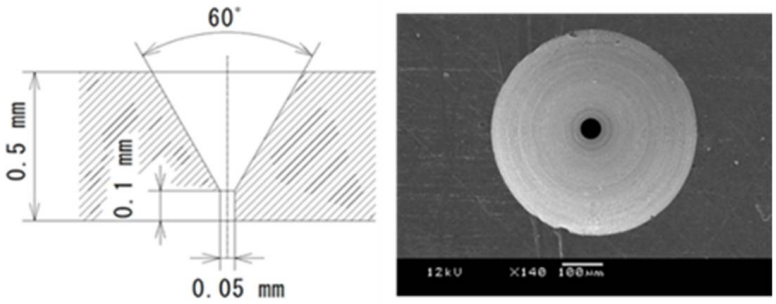

Figure 5. Schematic of lower micropore plate for core–shell droplet generation device: cross-sectional view of micropore (**left**) and SEM photograph of micropore (**right**).

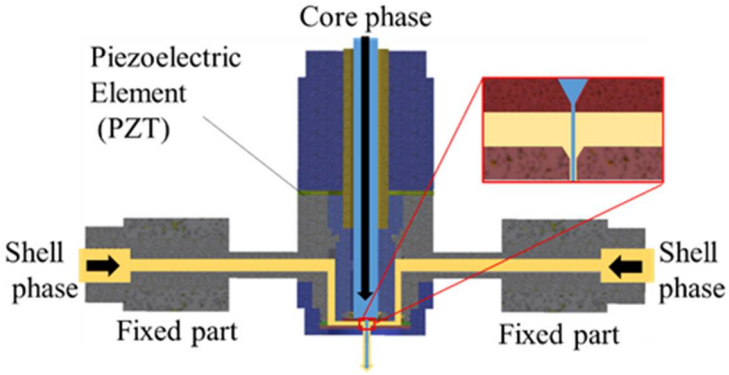

Figure 6. Fluid supply route for the core–shell droplet generation device under vibration mode.

2.3. Vibration Characteristics

This device was designed using finite element method analysis, as shown in Figure 7. The device was subjected to a first-order flexural vibration mode. The fixed part and the vibration node are at the same position; this design prevents vibration damping.

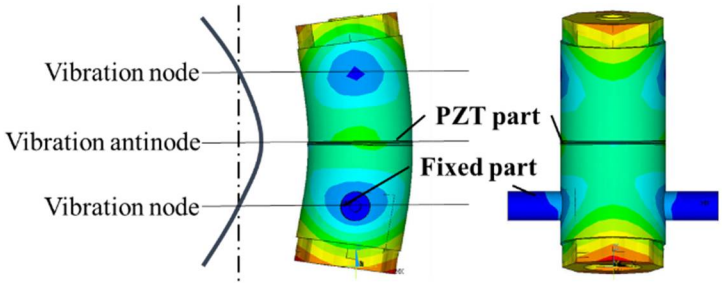

Figure 7. First-order flexural vibration of the device.

For alignment of the center of the upper and lower micropore plates, the micropores were placed at the center of each micropore plate. The flexural vibration is effective for oscillating the center of the micropore plate.

The relationship between frequency, admittance, and phase is shown in Figure 8. This device was designed to provide first-order flexural vibration at 30 kHz. The resonance frequency of the fabricated device was observed using a laser Doppler vibrometer at a frequency of 29 kHz.

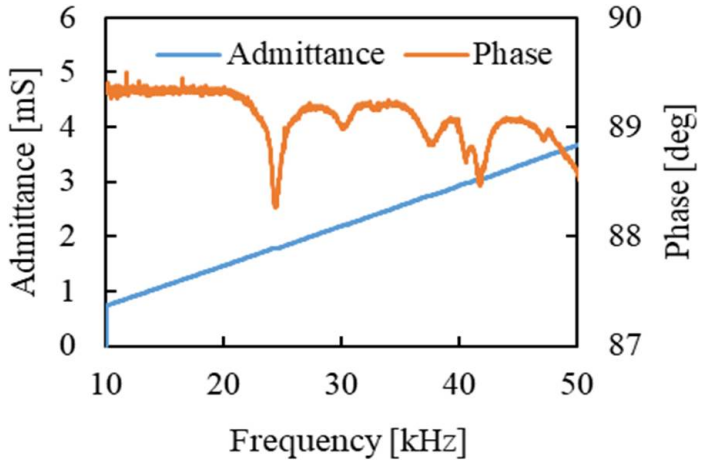

Figure 8. Relationship between frequency, admittance, and phase of the core–shell droplet generation device.

Figure 9 shows the relationship between distance from the tip of the core–shell droplet generation device and vibration velocity when the driving frequency and the voltage were 29 kHz and 100 $V_{p\text{-}p}$, respectively. Vibration nodes were observed at 9 and 33 mm; a vibrational antinode was observed at 21 mm, which corresponds to the center of the device. The results show that the device oscillated under a first-order flexural vibration mode.

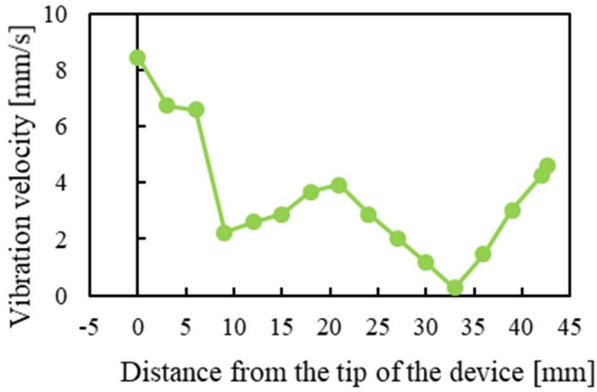

Figure 9. Relationship between the distance from the tip of the core–shell droplet generation device and the vibration velocity, when the driving frequency was 29 kHz.

Figure 10 shows the relationship between the applied voltage and the vibration velocity at the tip of the core–shell droplet generation device when the driving frequency was 29 kHz.

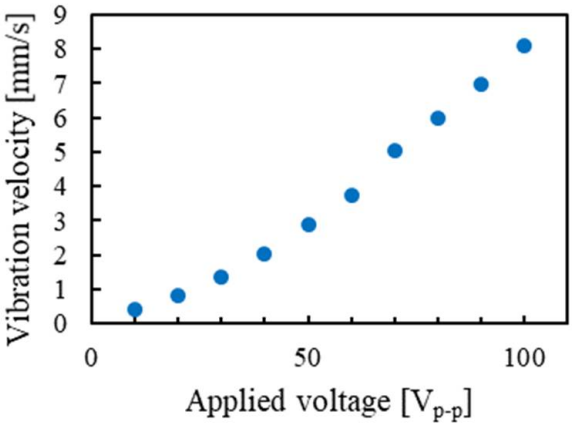

Figure 10. Relationship between the applied voltage and the vibration velocity, when the driving frequency was 29 kHz.

3. Results

3.1. System Configuration

Figure 11 shows the core–shell droplet generation experiment system. Core–shell droplets were generated in air when water and silicone oil (1 mm^2/s) were used as the core and shell phases, respectively. Core and shell phase fluids were supplied separately by applying pressure with a compressor and regulators. The vibration speed was controlled by the voltage and drive frequency applied to the piezoelectric element using a function generator and a high-speed bipolar power supply. The generated droplets were observed with a high-speed camera. The droplet diameter was measured using the image analysis software "WinROOF" (MITANI Corporation, Japan). One hundred droplets were measured for each type of experimental data.

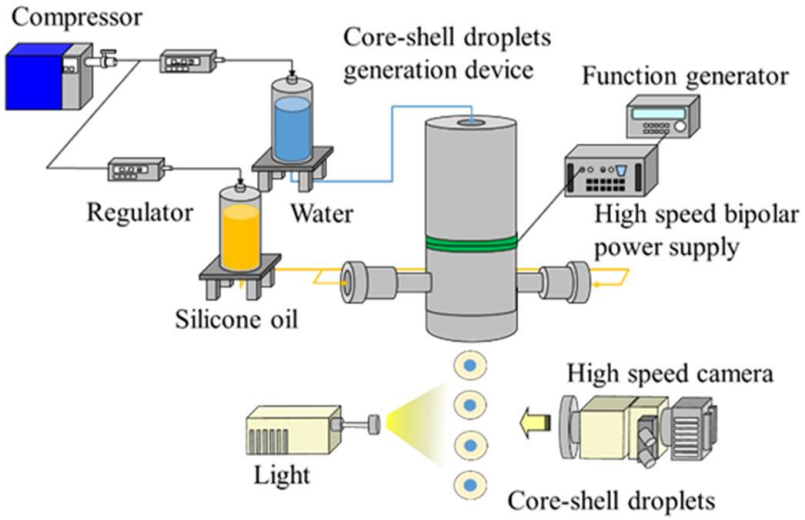

Figure 11. Core–shell droplet generation system.

In this research, monodispersity was assessed using the coefficient of variation. When the coefficient of variation was 5% or less, it was determined that a uniform droplet was generated.

3.2. Experiments with Varying Voltage

Core–shell droplets were generated when the applied voltage was changed. The applied pressures of the core and shell phases were 200 kPa and 150 kPa, respectively. The driving frequency was 29 kHz.

Figure 12 shows photographs of the generated core–shell droplets in the air when the applied voltages were 0, 6, 7, and 100 $V_{p\text{-}p}$. The vibration velocities of the micropore were 0, 0.12, 0.13, and 8.2 mm/s. Figure 13 shows the relationship between vibration velocity and the diameter of droplet. Table 1 shows the average droplet diameter when the applied voltage was changed. Figure 13 and Table 1 shows that monodisperse droplets were generated when the applied voltage was larger than 7 $V_{p\text{-}p}$.

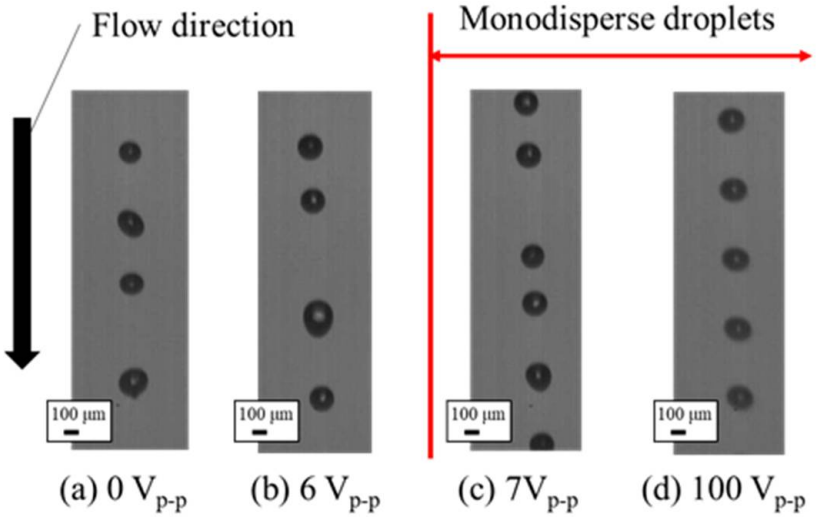

Figure 12. Photographs of generated core–shell droplets when the applied voltage was changed.

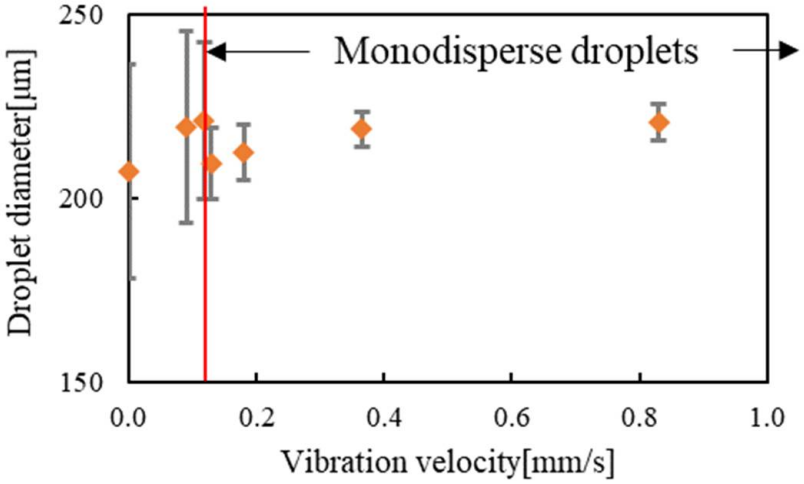

Figure 13. Relationship between vibration speed and droplet diameter when the driving frequency was 29 kHz and the applied pressure of core and shell phases were 200 kPa and 150 kPa.

Table 1. Average droplet diameter when the applied voltage was changed.

Applied voltage [$V_{p\text{-}p}$]	0	6	7	100
Vibration velocity [mm/s]	0	0.12	0.13	8.2
Average droplet diameter [μm]	207.3	221.2	209.4	207.7
Coefficient of variation [%]	14	9.7	4.7	1.6

3.3. Experiments with Varying Pressure

Core–shell droplets were generated by changing the applied pressure. The applied voltage was 100 $V_{p\text{-}p}$ and the drive frequency was 29 kHz.

Figure 14 shows photographs of the generated core–shell droplets in air when the applied pressure for the core phase was changed. Figure 15 shows the relationship between vibration velocity and droplet diameter. Table 2 shows average droplet diameter when the applied pressure for the core phase was changed. According to Table 2 monodisperse droplets were generated when the applied pressure was between 170 kPa and 320 kPa.

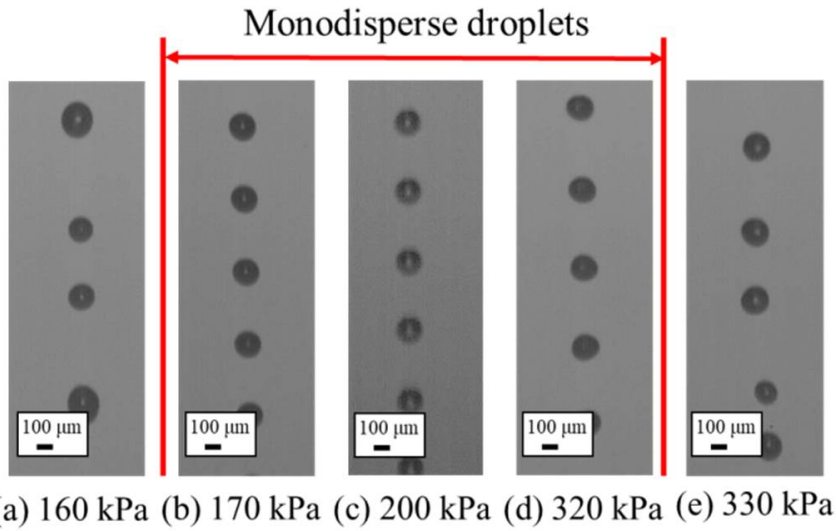

Figure 14. Photographs of generated core–shell droplets when the applied pressure was changed.

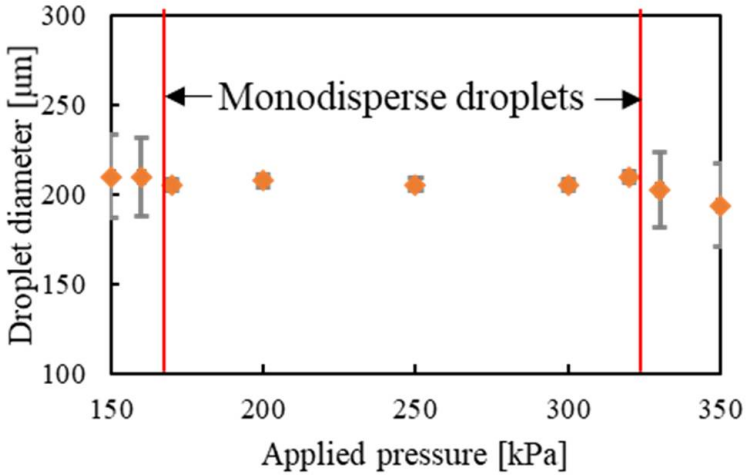

Figure 15. Relationship between applied pressure of the core phase and droplet diameter when the driving frequency was 29 kHz and the vibration velocity was 8.2 mm/s.

Table 2. Average droplet diameter when the applied pressure for the core phase was changed.

Applied pressure [kPa]	160	170	200	320	330
Average droplet diameter [μm]	209.8	205.4	207.7	209.7	202.8
Coefficient of variation [%]	10.4	1.6	1.6	1.4	10.3

4. Discussion

As shown in the experimental results, monodisperse core–shell droplets were generated by adjusting the applied voltage and the applied pressure. The voltage has a threshold value at which core–shell droplets can be generated. Because the applied voltage is almost proportional to the vibration velocity, the droplet generation requires a vibration velocity higher than the specified value.

There is a range of applied pressures at which core–shell droplets can be generated. The lower limit of the applied pressure is determined by the difference between the applied pressure of the core and shell phases ΔP. It is expressed by Equation (1)

$$\Delta P = 2\gamma/R_c > 2\gamma/R_o, \quad (1)$$

where γ is the interfacial tension between the core and shell phases, R_c is the spherical radius of the discharged core phase, and R_o is the radius of the lower micropore. When R_c is smaller than R_o, monodisperse droplets can be generated. In these experiments, γ was 41.6 mN/m and R_o was 0.05 mm. Therefore, ΔP was 16.6 kPa. When the applied pressure of the core phase was 160 kPa (ΔP = 10 kPa), generation of monodisperse droplets was impossible. When the applied pressure of the core phase was 170 kPa (ΔP = 20 kPa), monodisperse droplets could be generated.

The upper limit of the applied pressure is determined by the core–shell phase flow velocity v_{cs} and the core phase flow velocity v_c. The core–shell phase flow velocity is the flow velocity of the coaxial flow composed of the core and shell phases discharged from the lower micropore. The core phase flow velocity is the flow velocity of the core phase discharged from the upper micropore. When $v_{cs} > v_c$, droplet generation is possible. In Figure 16, the graph shows the relationship between the applied pressure of the core phase and the flow velocity. When the applied pressure of the core phase was 320 kPa, v_{cs} was 15.3 m/s, and v_c was 14.4 m/s, monodisperse droplets could be generated. When the applied pressure of the core phase was 330 kPa, v_{cs} was 15.3 m/s, and v_c was 15.3 m/s, generation of monodisperse droplets was impossible.

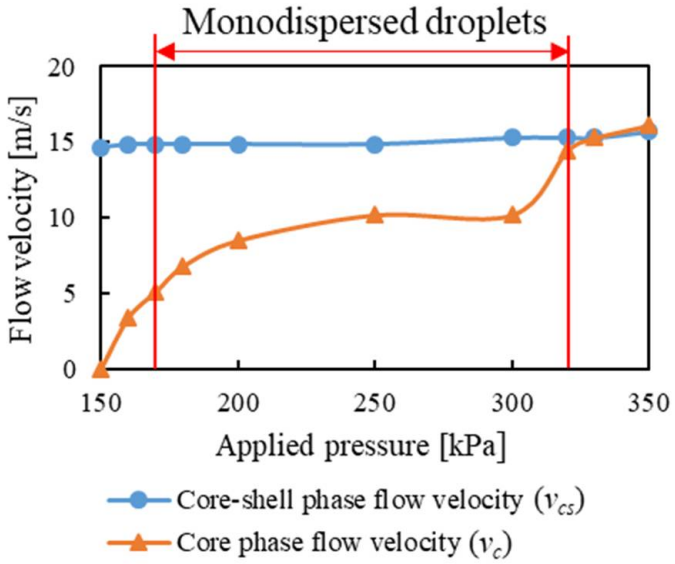

Figure 16. Relationship between applied pressure for core phase and flow velocity when the applied pressure for shell phase was 150 kPa.

Core–shell droplets were collected by ejecting water into a beaker. Figure 17 shows photographs of the collected core–shell droplets observed with an optical microscope. The water used in the core phase was colored blue. The water in the beaker was colored orange. Compared to the total number of generated droplets, fewer droplets were observed because many of them collapsed under the high flow velocity when they hit the water surface.

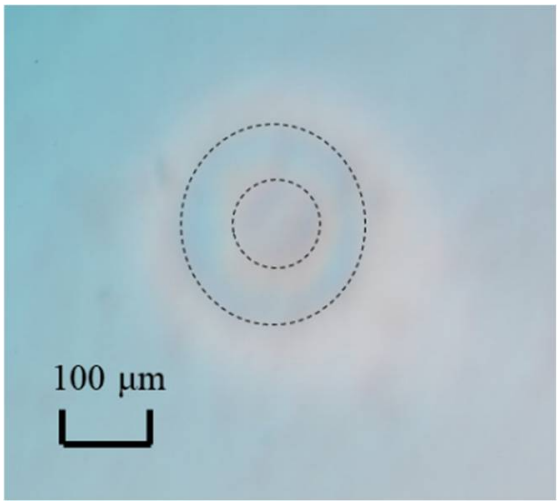

Figure 17. Relationship between applied pressure for core phase and flow velocity when the applied pressure for shell phase was 150 kPa.

5. Conclusions

Core–shell droplets were generated using flexural vibration. A core–shell droplet generation device was designed using a bolt-clamped Langevin-type flexural transducer and two micropore plates. The droplets were generated in air using water and silicone oil. A generation rate of 29,000 core–shell droplets per second was achieved. Monodisperse core–shell droplets were generated by adjusting the applied voltage and the applied pressure. The conditions of core-shell droplet generation were evaluated. We have succeeded in generating highly efficient and monodisperse core-shell droplets by using the ultrasonic transducer.

Author Contributions: Conceptualization, K.O., N.F. and T.K.; methodology, S.W. and N.S.; formal analysis, K.O. and N.F.; investigation, K.O. and N.F.; data curation, K.O.; writing—original draft preparation, K.O.; writing—review and editing, T.K.; visualization, K.O.; supervision, T.K.; project administration, T.K.; funding acquisition, T.K. All authors have read and agreed to the published version of the manuscript.

Funding: This research was partially supported by a grant for the Promotion of Science and Technology in Okayama Prefecture by NEXT.

Conflicts of Interest: The authors declare no conflict of interest.

References

1. Zhao, C. Multiphase flow microfluidics for the production of single or multiple emulsions for drug delivery. *Adv. Drug Deliv. Rev.* **2013**, *65*, 1420–1446. [CrossRef]
2. Chen, P.W.; Erb, R.M.; Studart, A.R. Designer Polymer-Based Microcapsules Made Using Microfluidics. *Langmuir* **2012**, *28*, 144–152. [CrossRef]
3. Zhu, Z.; Si, T.; Xu, R.X. Microencapsulation of indocyanine green for potential applications in image-guided drug delivery. *Lab Chip* **2015**, *15*, 646–649. [CrossRef] [PubMed]
4. Vericella, J.J.; Baker, S.E.; Stolaroff, J.K.; Duoss, E.B.; Iv, J.O.H.; Lewicki, J.; Glogowski, E.; Floyd, W.C.; Valdez, C.A.; Smith, W.L.; et al. Encapsulated liquid sorbents for carbon dioxide capture. *Nat. Commun.* **2015**, *6*, 6124. [CrossRef] [PubMed]
5. Zou, M.; Wang, J.; Yu, Y.; Sun, L.; Wang, H.; Xu, H.; Zhao, Y. Composite Multifunctional Micromotors from Droplet Micro-fluidics. *ACS Appl. Mater. Interfaces* **2018**, *10*, 34618–34624. [CrossRef]
6. Nakashima, T.; Shimizu, M.; Kukizaki, M. Particle Control of Emulsion by Membrane Emulsification and its Applications. *Adv. Drug Deliv. Rev.* **2000**, *45*, 47–56. [CrossRef]
7. Utada, A.S.; Lorenceau, E.; Link, D.R.; Kaplan, P.D.; Stone, H.A.; Weitz, D.A. Monodisperse Double Emulsions Generated from a Microcapillary Device. *Science* **2005**, *308*, 537–541. [CrossRef]
8. Zhao, C.-X.; Chen, D.; Hui, Y.; Weitz, D.A.; Middelberg, A.P.J. Controlled Generation of Ultrathin-Shell Double Emulsions and Studies on Their Stability. *ChemPhysChem* **2017**, *18*, 1–18. [CrossRef] [PubMed]
9. Nabavi, S.A.; Vladisavljević, G.T.; Gu, S.; Ekanem, E.E. Double Emulsion Production in Glass Capillary Microfluidic Device Parametric Investigation of Droplet Generation Behavior. *Chem. Eng. Sci.* **2015**, *130*, 183–196. [CrossRef]
10. Levenstein, M.A.; Bawazer, L.A.; Nally, C.S.M.; Marchant, W.J.; Gong, X.; Meldrum, F.C.; Kapur, N. A reproducible approach to the assembly of microcapillaries for double emulsion production. *Microfluid. Nanofluid.* **2016**, *20*, 143. [CrossRef]
11. Shi, W.; Didier, J.E.; Ingber, D.E.; Weitz, D.A. Collective Shape Actuation of Polymer Double Emulsions by Solvent Evaporation. *ACS Appl. Mater. Interfaces* **2018**, *10*, 31865–31869. [CrossRef]
12. Chen, Y.; Liu, X.; Shi, M. Hydrodynamics of double emulsion droplet in shear flow. *Appl. Phys. Lett.* **2013**, *102*, 051609. [CrossRef]
13. Chang, F.; Su, Y. Controlled double emulsification utilizing 3D PDMS microchannels. *J. Micromech. Microeng.* **2008**, *18*, 065018. [CrossRef]
14. Kong, L.; Levin, A.; Toprakcioglu, Z.; Xu, Y.; Gang, H.; Ye, R.; Mu, B.-Z.; Knowles, T.P.J. Lipid-Stabilized Double Emulsions Generated in Planar Microfluidic Devices. *Langmuir* **2020**, *36*, 2349–2356. [CrossRef]
15. Chang, Z.; Serra, C.A.; Bouquey, M.; Prat, L.; Hadziioannou, G. Co-axial capillaries microfluidic device for synthesizing size-and morphology-controlled polymer core-polymer shell particles. *Lab Chip* **2009**, *9*, 3007–3011. [CrossRef]
16. Zhu, Z.; Huang, F.; Yang, C.; Si, T.; Xu, R.X. On-Demand Generation of Double Emulsions Based on Interface Shearing for Controlled Ultrasound Activation. *ACS Appl. Mater. Interfaces* **2019**, *11*, 40932–40943. [CrossRef] [PubMed]
17. Song, Y.; Shum, H.C. Monodisperse w/w/w Double Emulsion Induced by Phase Separation. *Langmuir* **2012**, *28*, 12054–12059. [CrossRef] [PubMed]
18. Harada, T.; Ishikawa, N.; Kanda, T.; Suzumori, K.; Yamada, Y.; Sotowa, K.I. Droplet generation using a torsional Langevin-type transducer and a micropore plate. *Sens. Actuators A Phys.* **2009**, *155*, 168–174. [CrossRef]
19. Kishi, T.; Kiyama, Y.; Kanda, T.; Suzumori, K.; Seno, N. Microdroplet Generation Using an Ultrasonic Torsional Transducer Which has a Micropore with a Tapered Nozzle. *Arch. Appl. Mech.* **2016**, *82*, 1751–1762. [CrossRef]
20. Murakami, T.; Tominaga, Y.; Kanda, T.; Suzumori, K. Droplets Generation in the Flowing Ambient Liquid by Using an Ultrasonic Torsional Transducer. In Proceedings of the 2012 IEEE International Ultrasonics Symposium, Dresden, Germany, 7–10 October 2012; pp. 281–284.
21. Kiyama, Y.; Tominaga, Y.; Kanda, T.; Suzumori, K.; Kishi, T.; Yamada, Y.; Seno, N. Evaluation of Generated Micro Droplets Using Micropore Plates Oscillated by Ultrasonic Torsional Transducers. *Sens. Actuators A* **2012**, *185*, 92–100. [CrossRef]
22. Fujimoto, N.; Kanda, T.; Katsuta, M.; Sakata, Y.; Yamada, Y.; Seno, N.; Nakazaki, Y.; Otoyama, T. Nanoparticles generation using monodisperse droplets by an ultrasonic transducer. *Electron. Commun. Jpn.* **2020**, *103*, 49–55. [CrossRef]